

Hyper-density functional theory of soft matter

Florian Sammüller,¹ Silas Robitschko,¹ Sophie Hermann,¹ and Matthias Schmidt¹

¹*Theoretische Physik II, Physikalisches Institut, Universität Bayreuth, D-95447 Bayreuth, Germany*

(Dated: 12 March 2023)

We present a scheme for investigating arbitrary thermal observables in spatially inhomogeneous many-body systems. Extending the equilibrium ensemble yields any given observable as an explicit hyper-density functional. Associated local fluctuation profiles follow from an exact hyper-Ornstein-Zernike equation. Simulation-based supervised machine learning trains neural networks that act as hyper-direct correlation functionals which facilitate efficient and accurate predictions. We exemplify the approach for the cluster statistics of hard rods and square well particles. The theory provides access to complex order parameters, as is impossible in standard density functional theory.

Classical density functional theory is a powerful framework for describing the collective behaviour of a wide variety of relevant many-body systems [1–5]. Topical applications to soft matter [6] range from studies of hydrophobicity [7–11] to investigations of the molecular structure of liquids [11] and of electrolytes [12–14]. The central variable of density functional theory is the position-resolved one-body density profile. In recent developments, the local compressibility [8, 9, 15] and more general fluctuation profiles [16–18] were shown to be further useful indicators for collective phenomena, e.g. when systematically analyzing drying that occurs near substrates and around solutes [8, 9, 15, 18]. A further broad spectrum of observables, including recent multi-body correlation functions [19–21], are relevant for the study of complex systems.

The use of statistical mechanical sum rules [1, 4, 22, 23] is often decisive in the description of soft matter, as sum rules not only provide unambiguous consistency checks, but also as they encapsulate physical constraints, which ultimately facilitates to trace physical mechanisms and identify underlying causes for the emerging collective effects. Inline with further topical uses of the Noether theorem in Statistical Mechanics [24–30], the recent thermal Noether invariance theory [31–33] allows to systematically generate and classify a significant body of exact sum rules. The properties of general observables can be addressed via the recent hyperforce theory [33], which is similar in spirit to Hirschfelders’s hypervirial generalization [34] of the standard virial theorem [4].

Machine learning techniques see a rapidly increasing use in soft matter research across topics that range from characterization [35] to engineering of self-assembly [36], detection of colloidal structure [37], and the study of effective colloidal interaction potentials [38, 39]. In the context of density functional theory, machine learning was used for the construction of workable representations for the central functional both in the classical [40–50] and in the quantum realms [51–58]. The recent neural functional theory [48–50] constitutes a hybrid method that is based on many-body computer simulation data used to train a neural network, which then acts as a central numerical object that mirrors the functional structure prescribed by classical density functional theory.

Here we return to fundamentals and present a generalization of classical density functional theory that allows to investigate the behaviour of virtually arbitrary observables and their locally resolved fluctuation profiles. We specifically develop a general variational formalism based on an extended thermal ensemble and demonstrate that the relevant functional dependencies are amenable to supervised machine learning. We present model demonstrations for what we argue is a standalone and practically relevant computational scheme for the investigation of soft matter.

Density functional theory [1, 4] puts the one-body density distribution,

$$\rho(\mathbf{r}) = \langle \hat{\rho}(\mathbf{r}) \rangle, \quad (1)$$

at center stage. Here we have defined the one-body density “operator” in its standard form $\hat{\rho}(\mathbf{r}) = \sum_i \delta(\mathbf{r} - \mathbf{r}_i)$, with $\delta(\cdot)$ denoting the Dirac distribution, \mathbf{r} is a generic position variable, \mathbf{r}_i is the position of particle $i = 1, \dots, N$, and $\langle \cdot \rangle$ indicates the thermal average as specified below in detail. In the following we consider a general observable that is represented by a phasespace function $\hat{A}(\mathbf{r}^N)$, which in general depends on the position coordinates \mathbf{r}^N of all N particles, as well as possibly on additional parameters. Following its occurrence in the hyperforce theory [33] and in generalization of the one-body fluctuation profiles of Refs. [8, 9, 16–18], we consider a corresponding hyper-fluctuation profile $\chi_A(\mathbf{r})$ as the covariance of the density operator and the given observable. Together with the mean A we hence define:

$$A = \langle \hat{A} \rangle, \quad (2)$$

$$\chi_A(\mathbf{r}) = \text{cov}(\hat{\rho}(\mathbf{r}), \hat{A}), \quad (3)$$

where the covariance of two phasespace functions \hat{X} and \hat{Y} is given in the usual way as $\text{cov}(\hat{X}, \hat{Y}) = \langle \hat{X}\hat{Y} \rangle - \langle \hat{X} \rangle \langle \hat{Y} \rangle$, such that $\chi_A(\mathbf{r}) = \langle \hat{\rho}(\mathbf{r})\hat{A} \rangle - \rho(\mathbf{r})A$.

To be specific, we consider classical many-body systems of N particles of identical mass m . The Hamiltonian has the standard form $H = \sum_i \mathbf{p}_i^2 / (2m) + u(\mathbf{r}^N) + \sum_i V_{\text{ext}}(\mathbf{r}_i)$, where the sums run over all particles $i = 1, \dots, N$, the momentum of particle i is denoted by \mathbf{p}_i , the interparticle interaction potential is $u(\mathbf{r}^N)$, where

$\mathbf{r}^N \equiv \mathbf{r}_1, \dots, \mathbf{r}_N$ is a shorthand for all position coordinates, and $V_{\text{ext}}(\mathbf{r})$ is an external potential, here written as a function of the (generic) position coordinate \mathbf{r} . We work in the grand ensemble at absolute temperature T and chemical potential μ . The classical ‘‘trace’’ operation is defined as $\text{Tr} \cdot = \sum_{N=0}^{\infty} (h^{dN} N!)^{-1} \int d\mathbf{r}^N d\mathbf{p}^N \cdot$, where h denotes the Planck constant, d the spatial dimensionality, and $\int d\mathbf{r}^N d\mathbf{p}^N$ indicates the phasespace integral over all position coordinates and momenta of the system.

In order to incorporate the observable $\hat{A}(\mathbf{r}^N)$ into the framework, we consider an extended ensemble [59] that is here defined by the extended equilibrium many-body probability distribution $e^{-\beta(H-\mu N)+\lambda \hat{A}}/\Xi$, where λ is a coupling parameter that acts as a conjugate variable to $\hat{A}(\mathbf{r}^N)$; here $\beta = 1/(k_B T)$ with k_B denoting the Boltzmann constant. The extended grand partition sum is given as $\Xi = \text{Tr} e^{-\beta(H-\mu N)+\lambda \hat{A}}$ and the corresponding grand potential is $\Omega = -k_B T \ln \Xi$. Thermal averages are obtained via $\langle \cdot \rangle = \text{Tr} \cdot e^{-\beta(H-\mu N)+\lambda \hat{A}}/\Xi$. An alternative view of the extended ensemble can be based on rather considering an extended Hamiltonian $H_A = H - \lambda \hat{A}/\beta$ and formulating its associated standard grand ensemble. This formulation is equivalent to the above.

Despite the generalization we remain thereby only interested in the properties of the original system with Hamiltonian H , recovering its standard grand ensemble for the case of vanishing coupling constant, $\lambda \rightarrow 0$. Throughout we assume that $\hat{A}(\mathbf{r}^N)$ is of a form such that the statistical ensemble generated via H_A is well-defined in this limit and that indeed $H_A \rightarrow H$ recovers the original Hamiltonian.

The thermal average A and the hyper-fluctuation profile $\chi_A(\mathbf{r})$, as respectively defined via Eqs. (2) and (3), are generated via the following partial derivatives with respect to the coupling parameter λ :

$$A = -\frac{\partial \beta \Omega}{\partial \lambda}, \quad (4)$$

$$\chi_A(\mathbf{r}) = \frac{\partial \rho(\mathbf{r})}{\partial \lambda}. \quad (5)$$

The statepoint T, μ and the form of the external potential $V_{\text{ext}}(\mathbf{r})$ are thereby fixed upon differentiating. That Eqs. (4) and (5) hold can respectively be verified by elementary calculations taking into account that $-\beta \Omega = \ln \Xi$ and the definition (1) of $\rho(\mathbf{r})$. Equation (5) is also rapidly derived from the standard expression [1, 4] of the density profile as a functional derivative, $\delta \Omega / \delta V_{\text{ext}}(\mathbf{r}) = \rho(\mathbf{r})$, together with Eq. (3) and the recent [17] general identity $-\delta A / \delta \beta V_{\text{ext}}(\mathbf{r}) = \text{cov}(\hat{\rho}(\mathbf{r}), \hat{A}) = \chi_A(\mathbf{r})$. The latter relation is also straightforward to show by explicit calculation and it lends much physical meaning to $\chi_A(\mathbf{r})$ as the response function of the average A against changes in the shape of the scaled external potential $-\beta V_{\text{ext}}(\mathbf{r})$.

The Euler-Lagrange equation of classical density functional theory [1–4], applied to the extended Hamiltonian H_A , has the standard form:

$$c_1(\mathbf{r}, [\rho]) = \ln \rho(\mathbf{r}) + \beta V_{\text{ext}}(\mathbf{r}) - \beta \mu, \quad (6)$$

where $c_1(\mathbf{r}, [\rho])$ is the one-body direct correlation functional corresponding to H_A , i.e. for a system of particles that interact via the extended interparticle interaction potential $u(\mathbf{r}^N) - \lambda \hat{A}(\mathbf{r}^N)/\beta$. In Eq. (6) we have set the thermal de Broglie wavelength to unity and we denote functional dependence by square brackets throughout. As Eq. (6) holds for any value of λ , provided that $\rho(\mathbf{r})$ is the corresponding equilibrium density profile, we can differentiate the equation with respect to λ and retain a valid identity. The result is the following hyper-Ornstein-Zernike relation:

$$c_A(\mathbf{r}, [\rho]) = \frac{\chi_A(\mathbf{r})}{\rho(\mathbf{r})} - \int d\mathbf{r}' c_2(\mathbf{r}, \mathbf{r}', [\rho]) \chi_A(\mathbf{r}'). \quad (7)$$

The left hand side of Eq. (7) constitutes the hyper-direct correlation functional $c_A(\mathbf{r}, [\rho])$, as is obtained from parametrically differentiating the left hand side of Eq. (6) at fixed density profile:

$$c_A(\mathbf{r}, [\rho]) = \left. \frac{\partial c_1(\mathbf{r}, [\rho])}{\partial \lambda} \right|_{\rho}. \quad (8)$$

It remains to express the thermal expectation value A in the hyper-density functional framework. Instead of using its explicit average form (2), we turn to the relation (4) to express A via the parametric derivative of the extended grand potential, taken while keeping μ, T and the shape of $V_{\text{ext}}(\mathbf{r})$ fixed. Crucially, instead of considering explicit many-body expressions, we adopt the classical density functional perspective [1–5] in order to find the density functional $A[\rho]$. We hence work with the grand potential in its density functional form: $\Omega[\rho] = F_{\text{id}}[\rho] + F_{\text{exc}}[\rho] + \int d\mathbf{r} \rho(\mathbf{r}) [V_{\text{ext}}(\mathbf{r}) - \mu]$. Thereby the ideal gas free energy functional is $F_{\text{id}}[\rho] = k_B T \int d\mathbf{r} \rho(\mathbf{r}) [\ln \rho(\mathbf{r}) - 1]$ and $F_{\text{exc}}[\rho]$ denotes the excess (over ideal gas) free energy functional.

Differentiating $\Omega[\rho]$ with respect to λ at fixed $V_{\text{ext}}(\mathbf{r})$ gives one direct contribution and one term arising from the induced changes in $\rho(\mathbf{r})$. The latter term, $\int d\mathbf{r} \delta \Omega[\rho] / \delta \rho(\mathbf{r}) |_{V_{\text{ext}}} \partial \rho(\mathbf{r}) / \partial \lambda$, vanishes due to the stationarity of the grand potential, $\delta \Omega[\rho] / \delta \rho(\mathbf{r}) |_{V_{\text{ext}}} = 0$. The direct contribution is the derivative at fixed density, $-\partial \beta \Omega[\rho] / \partial \lambda |_{\rho} = -\partial \beta F_{\text{exc}}[\rho] / \partial \lambda |_{\rho}$, where we have exploited that the ideal, external and chemical potential contributions to $\Omega[\rho]$ are independent of λ . From recalling Eq. (4) we obtain $A[\rho] = -\partial \beta F_{\text{exc}}[\rho] / \partial \lambda |_{\rho}$.

Powerful methods of functional calculus allow us to re-write this formal expression for $A[\rho]$ as a functional integral [1, 2, 50]. Using the standard relation $c_1(\mathbf{r}, [\rho]) = -\delta \beta F_{\text{exc}}[\rho] / \delta \rho(\mathbf{r})$ together with the definition (8) of the hyper-direct correlation functional $c_A(\mathbf{r}, [\rho])$ gives:

$$c_A(\mathbf{r}, [\rho]) = \frac{\delta A[\rho]}{\delta \rho(\mathbf{r})}, \quad (9)$$

$$A[\rho] = \int \mathcal{D}[\rho] c_A(\mathbf{r}, [\rho]). \quad (10)$$

The functional derivative Eq. (9) gives much further significance to the hyper-direct correlation functional

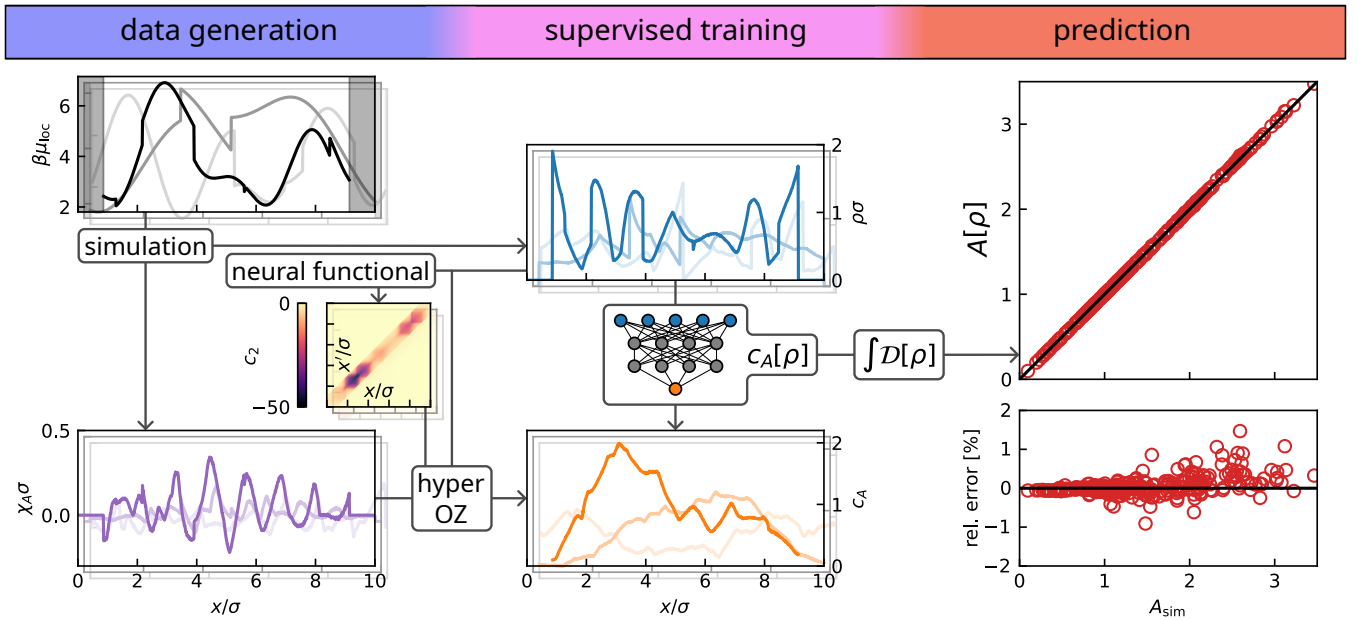


FIG. 1. Workflow of neural hyper-density functional theory. An exemplary choice of the observable \hat{A} is the size of the largest cluster in hard rods of size σ . Training data is generated from 512 grand canonical Monte Carlo simulations for randomized forms of the local chemical potential $\beta\mu_{\text{loc}}(x) = \beta\mu - \beta V_{\text{ext}}(x)$. Sampling yields the scaled hyper-fluctuation profile $\chi_A(x)\sigma$ via Eq. (3) (violet lines) and the scaled density profile $\rho(x)\sigma$ via Eq. (1) (blue lines). For each simulation run the hyper-direct correlation function $c_A(x)$ (orange lines) is obtained by solving Eq. (7) using the neural functional representation of the two-body direct correlation functional $c_2(x, x', [\rho])$ [49, 50]. Using the density profile as input and the values of $c_A(x)$ as output, supervised training yields a neural network that represents the hyper-direct correlation functional $c_A(x, [\rho])$. Functional integration gives the density functional $A[\rho] = \int D[\rho]c_A(x, [\rho])$ via Eq. (10). For a test set of 256 systems not encountered during training the predictions of $A[\rho]$ are compared against reference simulation data A_{sim} (red symbols). The relative numerical error of the predicted mean size A of the largest cluster is smaller than $\sim 1\%$.

$c_A(\mathbf{r}, [\rho])$ as measuring changes of the thermal mean A against local perturbation of the density profile $\rho(\mathbf{r})$. Equation (10) is the inverse of Eq. (9) upon standard functional integration [1, 2, 50]. One can efficiently parameterize the functional integral e.g. as $A[\rho] = \int d\mathbf{r}\rho(\mathbf{r}) \int_0^1 da c_A(\mathbf{r}, [a\rho])$, where the scaled density profile $a\rho(\mathbf{r})$ is obtained by multiplication of $\rho(\mathbf{r})$ with the parameter $0 \leq a \leq 1$. Very remarkably, Eq. (10) allows to express the thermal average of a given observable as an explicit density functional $A[\rho]$, provided that the density functional dependence of $c_A(\mathbf{r}, [\rho])$ is known.

As an initial test of this framework, we let the considered observable simply be the particle number, i.e. $\hat{A}(\mathbf{r}^N) = N$, which we recall is a fluctuating variable in the grand ensemble that we consider. According to Eq. (3) we have $\chi_A(\mathbf{r}) = \text{cov}(\hat{\rho}(\mathbf{r}), N)$ and from Eq. (4) we obtain $N = -\partial\beta\Omega/\partial\lambda$. Furthermore Eq. (5) yields $\chi_A(\mathbf{r}) = \partial\rho(\mathbf{r})/\partial\lambda$. These are all key properties of the local compressibility $\chi_\mu(\mathbf{r}) = \beta\chi_A(\mathbf{r})$ [8, 9, 15–18] with the coupling parameter λ playing the role of the scaled chemical potential $\beta\mu$. Turning to the density functional dependence, the hyper-direct correlation functional becomes constant unity, $c_A(\mathbf{r}, [\rho]) = 1$. As a consequence Eq. (7) reduces upon multiplication by $\rho(\mathbf{r})$ to: $\rho(\mathbf{r}) \int d\mathbf{r}' c_2(\mathbf{r}, \mathbf{r}', [\rho]) \chi_\mu(\mathbf{r}') + \beta\rho(\mathbf{r}) = \chi_\mu(\mathbf{r})$, which is the fluctuation Ornstein-Zernike relation [16, 17] for

the local compressibility $\chi_\mu(\mathbf{r})$. The functional integral (10) can be carried out explicitly with the result: $A[\rho] = \int d\mathbf{r}\rho(\mathbf{r}) \int_0^1 da = \int d\mathbf{r}\rho(\mathbf{r})$, where in the second step trivially $\int_0^1 da = 1$. The result for $A[\rho]$ is hence the mean number of particles, expressed as the density functional $\bar{N}[\rho] = \int d\mathbf{r}\rho(\mathbf{r})$, which certainly is correct due to $\int d\mathbf{r}\rho(\mathbf{r}) = \int d\mathbf{r}\langle\hat{\rho}(\mathbf{r})\rangle = \langle\int d\mathbf{r}\hat{\rho}(\mathbf{r})\rangle = \langle N \rangle = A$.

Having passed this initial test with nothing but flying colours we next address significantly more complex forms of \hat{A} . We therefore return to the hyper-Ornstein-Zernike equation (7) and consider the accessibility of the terms on its right hand side on the basis of direct simulations and the methods provided by the recent neural functional theory [49, 50].

Both the standard density profile $\rho(\mathbf{r})$ and the hyper-fluctuation profile $\chi_A(\mathbf{r})$ can be sampled for given μ, T , and $V_{\text{ext}}(\mathbf{r})$. We recall $\rho(\mathbf{r})$ as the average (1) and $\chi_A(\mathbf{r})$ as the covariance (3). For the given bare Hamiltonian H , the neural functional theory allows to construct a numerical representation of the direct correlation functional $c_1(\mathbf{r}, [\rho])$ as a neural network [49, 50]. Automatic differentiation then straightforwardly provides a numerically efficient and accurate neural functional representation of the two-body direct correlation functional $c_2(\mathbf{r}, \mathbf{r}', [\rho])$ which is ready for use in Eq. (7). Evaluating the right hand

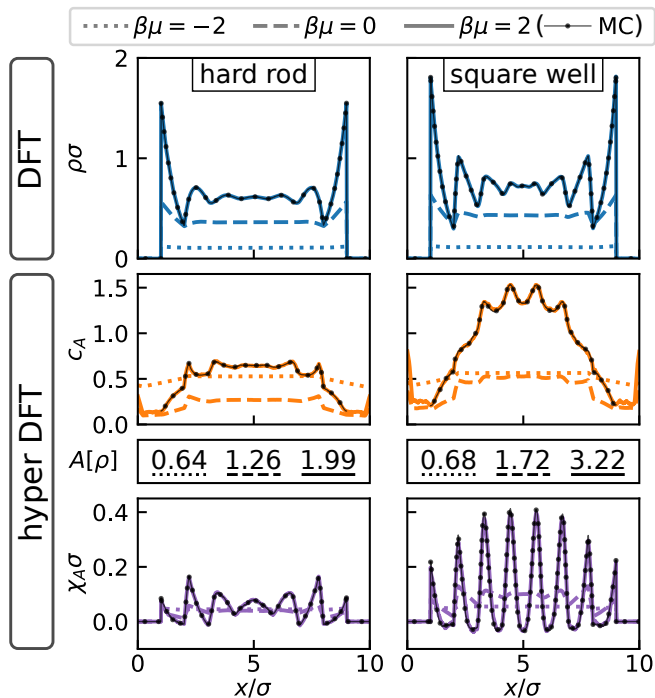


FIG. 2. Application of the hyper density functional theory to the statistics of the largest cluster of the hard rod and square well models. The systems are confined between two hard walls with separation distance $L = 10\sigma$ and the profiles are shown as a function of the scaled distance x/σ across the pore for $\beta\mu = -2$ (dotted), 0 (dashed), and 2 (solid lines). We depict theoretical results for the density profile $\rho(x)\sigma$ (blue), the hyper-direct correlation function $c_A(x)$ (orange), the mean value $A[\rho]$, and the hyper-fluctuation profile $\chi_A(x)\sigma$ (violet). For the case of largest density, Monte Carlo simulation results are shown as reference (black lines with symbols). These coincide with the respective theoretical predictions on the scale of the plot. The simulated reference values for A are identical within the quoted accuracy to the neural predictions $A[\rho]$.

side of Eq. (7) then only requires the numerical integration over \mathbf{r}' .

As for given μ, T , and $V_{\text{ext}}(\mathbf{r})$ the right hand side of Eq. (7) is hence explicitly accessible, the hyper-direct correlation function $c_A(\mathbf{r})$ that is specific for the considered inhomogeneous system can be computed. This facilitates the generation of a training data set from many-body simulation results. We do not invoke the functional dependence of $c_A(\mathbf{r}, [\rho])$ for this task yet and require only standard grand canonical Monte Carlo simulation techniques [60–62] with no need to implement the extended ensemble explicitly.

Following the neural methodology for standard density functionals [49, 50], this puts us in the position to establish via supervised machine learning the hyper-functional map

$$\rho(\mathbf{r}') \rightarrow c_A(\mathbf{r}), \quad (11)$$

where the density at positions \mathbf{r}' removed from \mathbf{r} will contribute with a range of non-locality that is specific to the

form of the observable $\hat{A}(\mathbf{r}^N)$. We proceed in analogy to Refs. [49, 50] in constructing a neural network representation of $c_A(\mathbf{r}, [\rho])$ via supervised machine learning on the basis of randomized training data sets, where at fixed temperature T , the value of μ and the shape of $V_{\text{ext}}(\mathbf{r})$ are varied. An illustration of the principal workflow is shown in Fig. 1 as applied to the following physical setup.

We choose one-dimensional systems with either pure hard core interactions or an additional square well attraction. Despite the availability of Percus' exact free energy functional for the former model [63, 64] we solely work on the basis of neural functionals, which were shown to match the Percus solution to high accuracy [50]. The density profile under the influence of an external potential hence follows from numerical solution of the Euler-Lagrange equation (6) for $\lambda = 0$, using the respective neural one-body direct correlation functional. As a model order parameter with genuine many-body character, we investigate cluster properties and therefore define two particles i and j as bonded if their (one-dimensional) positions x_i and x_j are within a bonding cutoff, $|x_i - x_j| < x_c$, where we choose $x_c = 1.2\sigma$, with the hard core particle diameter σ . For each microstate of positions $x^N = x_1, \dots, x_N$, we construct an instantaneous histogram that gives the number of clusters with (integer) size m , where a cluster consists of all particles that are bonded directly or mediated by other bonded particles. This is a standard criterion that is independent of dimensionality and used in studies of gelation, see e.g. Ref. [65].

Specifically we choose \hat{A} as the size of the largest cluster that is present in a given microstate. Although one-dimensional hard cores have no intrinsic propensity to cluster, we find this setup a crucial test, as there is no way to assess the statistical properties via conventional density functional methods. Exemplary profiles are shown in Fig. 1 together with the numerical predictions from the neural functional $A[\rho]$, as evaluated via the functional integral (10). The neural predictions are highly accurate with a consistent relative error below $\sim 1\%$ as compared to the simulation reference.

On the basis of the availability of the neural hyper-direct correlation functional we can formulate a template for standalone application of the hyper-density functional theory, with no reliance on further simulation data. We require trained neural network representations for $c_A(\mathbf{r}, [\rho])$ and for $c_1(\mathbf{r}, [\rho])$. Automatic functional differentiation of the latter yields a neural representation of $c_2(\mathbf{r}, \mathbf{r}', [\rho])$. In a prototypical study of inhomogeneous states of a given model fluid, the behaviour of the target observable A is of interest when the system is under the influence of a prescribed external potential $V_{\text{ext}}(\mathbf{r})$.

First, in a conventional density functional setting the solution of the Euler-Lagrange equation (6) at given μ, T yields the shape of the equilibrium density profile $\rho(\mathbf{r})$. This form is then used to evaluate the hyper-direct correlation functional $c_A(\mathbf{r}, [\rho])$ and the two-body direct correlation functional $c_2(\mathbf{r}, \mathbf{r}', [\rho])$. The resulting functions

turn the hyper-direct Ornstein-Zernike relation (7) into a concrete integral equation for determining the hyper-fluctuation profile $\chi_A(\mathbf{r})$. Predictions for the mean value A in the considered system are obtained from calculating $A[\rho]$ at the known equilibrium density profile via numerical evaluation of the functional integral (10).

Figure 2 shows results from this strategy applied to the cluster statistics of both the hard rod and square-well system (potential range 0.2σ and depth $\beta\epsilon = 1$) [66]. We consider confinement between two hard walls, but with no further disturbing influence as was present dur-

ing training. This clean situation tests the genuine extrapolation capability of the neural functionals. The results shown in Fig. 2 achieve excellent agreement with reference simulation data. This successful application demonstrates that we have developed a systematic functional approach that allows to address the equilibrium behaviour of general observables. The statistical mechanical many-body problem is thereby cast into functional form, which we have shown to be accessible via simulation-based training of neural networks that can be applied efficiently in accomplishing predictive tasks.

-
- [1] R. Evans, The nature of the liquid-vapour interface and other topics in the statistical mechanics of non-uniform, classical fluids, *Adv. Phys.* **28**, 143 (1979).
- [2] R. Evans, Density functionals in the theory of nonuniform fluids, Chap. 3 in *Fundamentals of Inhomogeneous Fluids*, edited by D. Henderson (Dekker, New York, 1992).
- [3] R. Evans, M. Oettel, R. Roth, and G. Kahl, New developments in classical density functional theory, *J. Phys.: Condens. Matter* **28**, 240401 (2016).
- [4] J. P. Hansen and I. R. McDonald, *Theory of Simple Liquids*, 4th ed. (Academic Press, London, 2013).
- [5] M. Schmidt, Power functional theory for many-body dynamics, *Rev. Mod. Phys.* **94**, 015007 (2022).
- [6] R. Evans, D. Frenkel, and M. Dijkstra, From simple liquids to colloids and soft matter, *Phys. Today* **72**, 38 (2019).
- [7] M. Levesque, R. Vuilleumier, and D. Borgis, Scalar fundamental measure theory for hard spheres in three dimensions: Application to hydrophobic solvation, *J. Chem. Phys.* **137**, 034115 (2012).
- [8] R. Evans and M. C. Stewart, The local compressibility of liquids near non-adsorbing substrates: a useful measure of solvophobicity and hydrophobicity?, *J. Phys.: Condens. Matter* **27**, 194111 (2015).
- [9] R. Evans, M. C. Stewart, and N. B. Wilding, A unified description of hydrophilic and superhydrophobic surfaces in terms of the wetting and drying transitions of liquids, *Proc. Natl. Acad. Sci.* **116**, 23901 (2019).
- [10] M. K. Coe, R. Evans, and N. B. Wilding, Density depletion and enhanced fluctuations in water near hydrophobic solutes: identifying the underlying physics, *Phys. Rev. Lett.* **128**, 045501 (2022).
- [11] G. Jeanmairet, M. Levesque, and D. Borgis, Molecular density functional theory of water describing hydrophobicity at short and long length scales. *J. Chem. Phys.* **139**, 154101 (2013).
- [12] D. Martin-Jimenez, E. Chacón, P. Tarazona, and R. Garcia, Atomically resolved three-dimensional structures of electrolyte aqueous solutions near a solid surface, *Nat. Commun.* **7**, 12164 (2016).
- [13] J. Hernández-Muñoz, E. Chacón, and P. Tarazona, Density functional analysis of atomic force microscopy in a dense fluid, *J. Chem. Phys.* **151**, 034701 (2019).
- [14] P. Cats, R. Evans, A. Härtel, and R. van Roij, Primitive model electrolytes in the near and far field: Decay lengths from DFT and simulations, *J. Chem. Phys.* **154**, 124504 (2021).
- [15] N. B. Wilding, R. Evans, and F. Turci, What is the best simulation approach for measuring local density fluctuations near solvo/hydrophobes? arXiv:2402.05692.
- [16] T. Eckert, N. C. X. Stuhlmüller, F. Sammüller, and M. Schmidt, Fluctuation profiles in inhomogeneous fluids, *Phys. Rev. Lett.* **125**, 268004 (2020).
- [17] T. Eckert, N. C. X. Stuhlmüller, F. Sammüller, and M. Schmidt, Local measures of fluctuations in inhomogeneous liquids: Statistical mechanics and illustrative applications, *J. Phys.: Condens. Matter* **35**, 425102 (2023).
- [18] M. K. Coe, R. Evans, and N. B. Wilding, Understanding the physics of hydrophobic solvation, *J. Chem. Phys.* **158**, 034508 (2023).
- [19] Z. Zhang and W. Kob, Revealing the three-dimensional structure of liquids using four-point correlation functions, *Proc. Natl. Acad. Sci.* **117**, 14032 (2020).
- [20] N. Singh, Z. Zhang, A. K. Sood, W. Kob, and R. Ganapathy, Intermediate-range order governs dynamics in dense colloidal liquids, *Proc. Natl. Acad. Sci.* **120**, e2300923120 (2023).
- [21] I. Pihlajamaa, C. C. L. Laudicina, C. Luo, L. M. C. Janssen, Emergent structural correlations in dense liquids, *PNAS Nexus* **2**, pgad184 (2023).
- [22] R. Evans and A. O. Parry, Liquids at interfaces: what can a theorist contribute? *J. Phys.: Condens. Matter* **2**, SA15 (1990).
- [23] J. R. Henderson, Statistical mechanical sum rules, Chap. 2 in *Fundamentals of Inhomogeneous Fluids*, edited by D. Henderson (Dekker, New York, 1992).
- [24] M. Revzen, Functional integrals in statistical physics, *Am. J. Phys.* **38**, 611 (1970).
- [25] I. Marvian and R. W. Spekkens, Extending Noether's theorem by quantifying the asymmetry of quantum states, *Nat. Commun.* **5**, 3821 (2014).
- [26] S. Sasa and Y. Yokokura, Thermodynamic entropy as a Noether invariant, *Phys. Rev. Lett.* **116**, 140601 (2016).
- [27] S. Sasa, S. Sugiura, and Y. Yokokura, Thermodynamical path integral and emergent symmetry, *Phys. Rev. E* **99**, 022109 (2019).
- [28] Y. A. Budkov and A. L. Kolesnikov, Modified Poisson-Boltzmann equations and macroscopic forces in inhomogeneous ionic fluids, *J. Stat. Mech.* **2022**, 053205 (2022).
- [29] P. E. Brandyshev and Y. A. Budkov, Noether's second theorem and covariant field theory of mechanical stresses in inhomogeneous ionic fluids, *J. Chem. Phys.* **158**, 174114 (2023).

- [30] A. Bravetti, M. A. Garcia-Ariza, and D. Tapias, Thermodynamic entropy as a Noether invariant from contact geometry, *Entropy* **25**, 1082 (2023).
- [31] S. Hermann and M. Schmidt, Noether's theorem in statistical mechanics, *Commun. Phys.* **4**, 176 (2021).
- [32] S. Hermann and M. Schmidt, Why Noether's theorem applies to statistical mechanics, *J. Phys.: Condens. Matter* **34**, 213001 (2022) (Topical Review).
- [33] S. Robitschko, F. Sammüller, M. Schmidt, and S. Hermann, Hyperforce balance and reverse engineering of thermal Noether invariance of any observable, *Commun. Phys.* (to appear) arxiv:2308.12098.
- [34] J. O. Hirschfelder, Classical and quantum mechanical hypervirial theorems, *J. Chem. Phys.* **33**, 1462 (1960).
- [35] P. S. Clegg, Characterising soft matter using machine learning, *Soft Matter*, **17**, 3991 (2021).
- [36] M. Dijkstra and E. Luijten, From predictive modelling to machine learning and reverse engineering of colloidal self-assembly, *Nat. Mater.* **20**, 762 (2021).
- [37] E. Boattini, M. Dijkstra, and L. Filion, Unsupervised learning for local structure detection in colloidal systems, *J. Chem. Phys.* **151**, 154901 (2019).
- [38] G. Campos-Villalobos, E. Boattini, L. Filion, and M. Dijkstra, Machine learning many-body potentials for colloidal systems, *J. Chem. Phys.* **155**, 174902 (2021).
- [39] G. Campos-Villalobos, G. Giunta, S. Marín-Aguilar, and M. Dijkstra, Machine-learning effective many-body potentials for anisotropic particles using orientation-dependent symmetry functions, *J. Chem. Phys.* **157**, 024902 (2022).
- [40] T. Santos-Silva, P. I. C. Teixeira, C. Anquetil-Deck, and D. J. Cleaver, Neural-network approach to modeling liquid crystals in complex confinement, *Phys. Rev. E* **89**, 053316 (2014).
- [41] S.-C. Lin and M. Oettel, A classical density functional from machine learning and a convolutional neural network, *SciPost Phys.* **6**, 025 (2019).
- [42] S.-C. Lin, G. Martius, and M. Oettel, Analytical classical density functionals from an equation learning network, *J. Chem. Phys.* **152**, 021102 (2020).
- [43] P. Cats, S. Kuipers, S. de Wind, R. van Damme, G. M. Coli, M. Dijkstra, and R. van Roij, Machine-learning free-energy functionals using density profiles from simulations, *APL Mater.* **9**, 031109 (2021).
- [44] C. Qiao, X. Yu, X. Song, T. Zhao, X. Xu, S. Zhao, and K. E. Gubbins, Enhancing gas solubility in nanopores: a combined study using classical density functional theory and machine learning, *Langmuir* **36**, 8527 (2020).
- [45] P. Yatsyshin, S. Kalliadasis, and A. B. Duncan, Physics-constrained Bayesian inference of state functions in classical density-functional theory, *J. Chem. Phys.* **156**, 074105 (2022).
- [46] A. Malpica-Morales, P. Yatsyshin, M. A. Duran-Olivencia, and S. Kalliadasis, Physics-informed Bayesian inference of external potentials in classical density functional theory, *J. Chem. Phys.* **159**, 104109 (2023).
- [47] X. Fang, M. Gu and J. Wu, Reliable emulation of complex functionals by active learning with error control, *J. Chem. Phys.* **157**, 214109 (2022).
- [48] D. de las Heras, T. Zimmermann, F. Sammüller, S. Hermann, and M. Schmidt, Perspective: How to overcome dynamical density functional theory, *J. Phys.: Condens. Matter* **35**, 271501 (2023). (Invited Perspective).
- [49] F. Sammüller, S. Hermann, D. de las Heras, and M. Schmidt, Neural functional theory for inhomogeneous fluids: Fundamentals and applications, *Proc. Natl. Acad. Sci.* **120**, e2312484120 (2023).
- [50] F. Sammüller, S. Hermann, and M. Schmidt, Why neural functionals suit statistical mechanics, *J. Phys.: Condens. Matter (Topical Review)* doi:10.1088/1361-648X/ad326f, arXiv:2312.04681.
- [51] R. Nagai, R. Akashi, S. Sasaki, and S. Tsuneyuki, Neural-network Kohn-Sham exchange-correlation potential and its out-of-training transferability, *J. Chem. Phys.* **148**, 241737 (2018).
- [52] J. Schmidt, C. L. Benavides-Riveros, and M. A. L. Marques, Machine learning the physical nonlocal exchange-correlation functional of density-functional theory, *J. Phys. Chem. Lett.* **10**, 6425 (2019).
- [53] Y. Zhou, J. Wu, S. Chen, and G. Chen, Toward the exact exchange-correlation potential: A three-dimensional convolutional neural network construct, *J. Phys. Chem. Lett.* **10**, 7264 (2019).
- [54] R. Nagai, R. Akashi, and O. Sugino, Completing density functional theory by machine learning hidden messages from molecules, *npj Comput. Mater.* **6**, 43 (2020).
- [55] L. Li, S. Hoyer, R. Pederson, R. Sun, E. D. Cubuk, P. Riley, and K. Burke, Kohn-Sham equations as regularizer: Building prior knowledge into machine-learned physics, *Phys. Rev. Lett.* **126**, 036401 (2021).
- [56] H. Li, N. Zou, M. Ye, R. Xu, X. Gong, and W. Duan, Deep-learning density functional theory Hamiltonian for efficient ab initio electronic-structure calculation, *Nat. Comput. Sci.* **2**, 367 (2022).
- [57] J. Gedeon, J. Schmidt, M. J. P. Hodgson, J. Wetherell, C. L. Benavides-Riveros, and M. A. L. Marques, Machine learning the derivative discontinuity of density-functional theory, *Mach. Learn.: Sci. Technol.* **3**, 015011 (2022).
- [58] R. Pederson, B. Kalita, and K. Burke, Machine learning and density functional theory, *Nat. Rev. Phys.* **4**, 357 (2022).
- [59] See, e.g., R. Zwanzig, *Nonequilibrium Statistical Mechanics* (Oxford University Press, Oxford, 2001).
- [60] D. Frenkel and B. Smit, *Understanding Molecular Simulation: From Algorithms to Applications*, 3rd ed. (Academic Press, London, 2023).
- [61] N. B. Wilding, Computer simulation of fluid phase transitions, *Am. J. Phys.* **69**, 1147 (2001).
- [62] A. V. Brukhno, J. Grant, T. L. Underwood, K. Stratford, S. C. Parker, J. A. Purton, and N. B. Wilding, DL_MONTE: a multipurpose code for Monte Carlo simulation, *Molec. Simul.* **47**, 131 (2021).
- [63] J. K. Percus, Equilibrium state of a classical fluid of hard rods in an external field, *J. Stat. Phys.* **15**, 505 (1976).
- [64] A. Robledo and C. Varea, On the relationship between the density functional formalism and the potential distribution theory for nonuniform fluids, *J. Stat. Phys.* **26**, 513 (1981).
- [65] F. Sammüller, D. de las Heras, and M. Schmidt, Inhomogeneous steady shear dynamics of a three-body colloidal gel former, *J. Chem. Phys.* **158**, 054908 (2023). (Special Topic on Colloidal Gels).
- [66] Source code, simulation data, and neural functionals are available at: <https://github.com/sfalmo/HyperDFT>.